1 December 1998

Optics Communications 157 (1998) 57–61

OPTICS COMMUNICATIONS

Automated spatial and temporal shaping of femtosecond pulses

Richard M. Koehl *, Toshiaki Hattori [1], Keith A. Nelson

Department of Chemistry, Massachusetts Institute of Technology, Cambridge, MA 02139, USA

Received 5 August 1998; accepted 9 September 1998

Abstract

The use of a liquid crystal spatial light modulator for the simultaneous spatial and temporal shaping of ultrafast optical pulses is demonstrated. A commercially available liquid crystal mask filters spatially dispersed frequency components in the horizontal direction, and spatial (or wavevector) components in the vertical direction. As an illustration, a coherent pulse sequence with nine spatial features and two temporal features per spatial feature is produced.

Keywords: Automated; Spatial and temporal shaping; Femtosecond pulses

The area of femtosecond pulse shaping has advanced dramatically in the past several years, motivated by applications in optical control over molecules and materials and in optical processing applications. In most cases, a single incident beam consisting of a single femtosecond pulse is transformed into a single outgoing beam consisting of femtosecond pulse sequence or other 'shaped' waveform whose time-dependent amplitude and phase profiles are specified. Femtosecond pulse shaping technology [1–12] has advanced to the point that high-resolution computer-controlled temporal waveform shaping of coherent pulses (and even incoherent noise [5]) is readily achievable [7–11].

Recently, examples have been reported in which both spatial and temporal properties of the shaped waveform have been specified [1,2]. The combination of simultaneous spatial and temporal shaping gives an additional degree of freedom for multiplexing in optical processing applications or for attempting to manipulate propagating excitations in crystals and other hosts [13]. In spatiotemporal shaping, a single incident beam consisting of a single femtosecond pulse can be transformed into many separate outgoing beams, each of which consists of an independently specified pulse sequence or other temporally 'shaped' waveform. More broadly, the result should be thought of as a single output whose position-dependent as well as time-dependent amplitude and phase profiles can be specified. An alternate but equivalent view is in terms of shaping of the wavevector content rather than the spatial profile. As a simple example, the output may consist of two separate beams or, after a focusing element, may consist of an interference pattern resulting from the intersection of those beams in the focal plane. Thus depending on how the output is imaged and where it is viewed, a description in terms of wavevector or position-dependent features may be more convenient. Related applications such as space to time conversion [2] and dynamic spectral holography via multiple quantum wells [12] have been demonstrated.

Here, we report preliminary results demonstrating the automation and computer control of spatiotemporal pulse shaping. The objective is to be able to specify the desired temporal and spatial (or wavevector) features and have those features generated automatically, with no further user involvement. This level of automation is essential for realization of the potential of spatiotemporal shaping for a very wide range of applications. Although the properties of the crucial optical element do not yet permit this result for

* Corresponding author. E-mail: rkoehl@mit.edu

[1] Permanent address: Institute of Applied Physics, University of Tsukuba, Tsukuba, Ibaraki 305, Japan.

0030-4018/98/$ - see front matter
PII: S0030-4018(98)00486-6

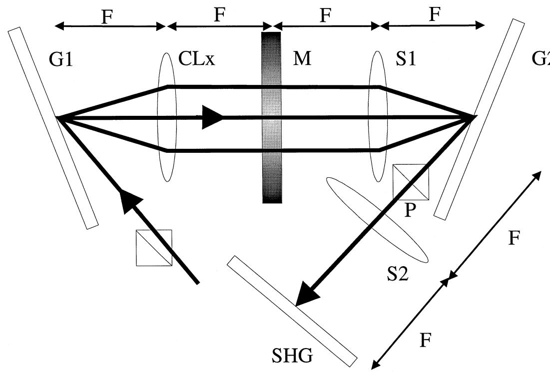

Fig. 1. Apparatus used for programmable generation of multidimensional shaped optical waveforms. A horizontally polarized short pulse incident on grating G1 (1200 lines/mm, angle 39°10′) is dispersed into frequency components along the x axis and focused by cylindrical lens CLx (focal length $F=20$ cm, curvature along the x axis into the page) onto the multidimensional mask M. Following filtering by M, the frequency components are focused by spherical lens S1 onto grating G2 (antiparallel to G1) and recombined into a sequence of short pulses. A second spherical lens S2 forms a 1:1 telescope in the vertical (spatial shaping) direction with S1 and focuses the horizontal component of the temporally and spatially shaped beam to its minimum width at second harmonic generation crystal SHG, where it may be cross-correlated with an unshaped, cylindrically focused reference beam (not shown).

a sufficiently wide range of waveforms, the present results clearly demonstrate that the possibility will be realized and indicate the steps necessary to reach it.

The spatiotemporal pulse shaping setup, similar to that reported earlier, is illustrated in Fig. 1. A horizontally polarized, 80-fs pulse from a kHz amplified Ti:sapphire laser is diffracted off a 1200 lines/mm sinusoidal grating so that its frequency components are spatially separated in the horizontal direction. An $f=20$ cm cylindrical lens, placed one focal length from the first grating and having its curvature in the horizontal direction, focuses the separated frequency components onto a mask which is placed one focal length behind the cylindrical lens. Since there is no focusing in the vertical direction, each frequency component extends along a vertical line in the focal plane, with the different frequency components separated horizontally. The mask contains a spatially varying two-dimensional pattern which can be used as a spatially varying amplitude and/or phase filter of selected frequency components, as described further below. After the mask, an $f=20$ cm spherical lens refocuses the spatially separated frequency components onto a second 1200 lines/mm sinusoidal grating. The first and second gratings are antiparallel, so that after the second grating, all frequency components once again travel the same path. The vertical spatial components are also focused by the second lens but are unaffected by the second grating. A second $f=20$ cm spherical lens placed one focal length after the second grating forms a 1:1 telescope in the vertical direction with the first spherical lens, yielding collimation of the shaped output in the vertical direction, and focuses the output along the horizontal direction, yielding a vertical line of light at the focal plane. This output is shaped spatially along the vertical direction, and each region of light along this direction is shaped temporally in a manner independent from each other region. The shaped output can be cross-correlated with a variably delayed, unshaped pulse that is cylindrically focused to a similar vertical line, with the shaped and unshaped lines of light spatially coincident inside a thin second harmonic generator. The frequency-doubled light is imaged onto a CCD detector. A 20-μJ pulse with central wavelength of 787 nm was split to generate both the

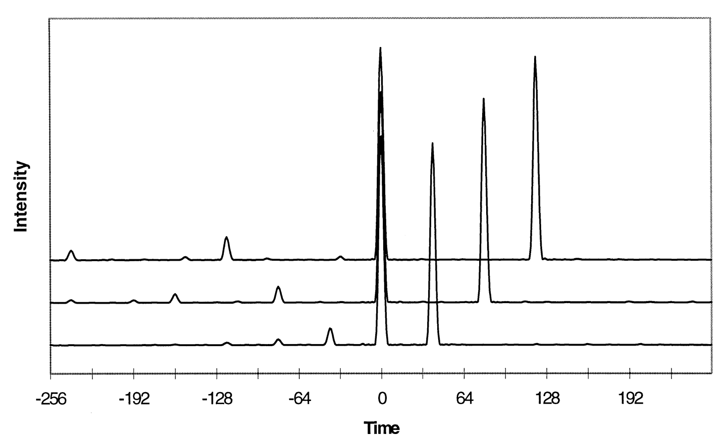

Fig. 2. Theoretical two-pulse sequences generated by simulated annealing. The second pulse is delayed by (from bottom to top) 40, 80, and 120 units out of 512 arbitrary temporal units. Although 512 points were used for the Fourier transform, this calculation was based on only a 128-point mask. The extra points were used to model the bandwidth distribution on the mask, assumed to be Gaussian [3]. The small replica pulses that appear on the other side of the zero-order temporal diffraction peak (at $t=0$) are unavoidable, given the constraints of the masks, as discussed in the text.

shaped waveform (12 μJ incident into the shaper, approximately 2μJ output) and the unshaped reference pulse (8 μJ).

The setup used here differs from that used for conventional temporal-only shaping in which the first lens is spherical rather than cylindrical and the mask is spatially

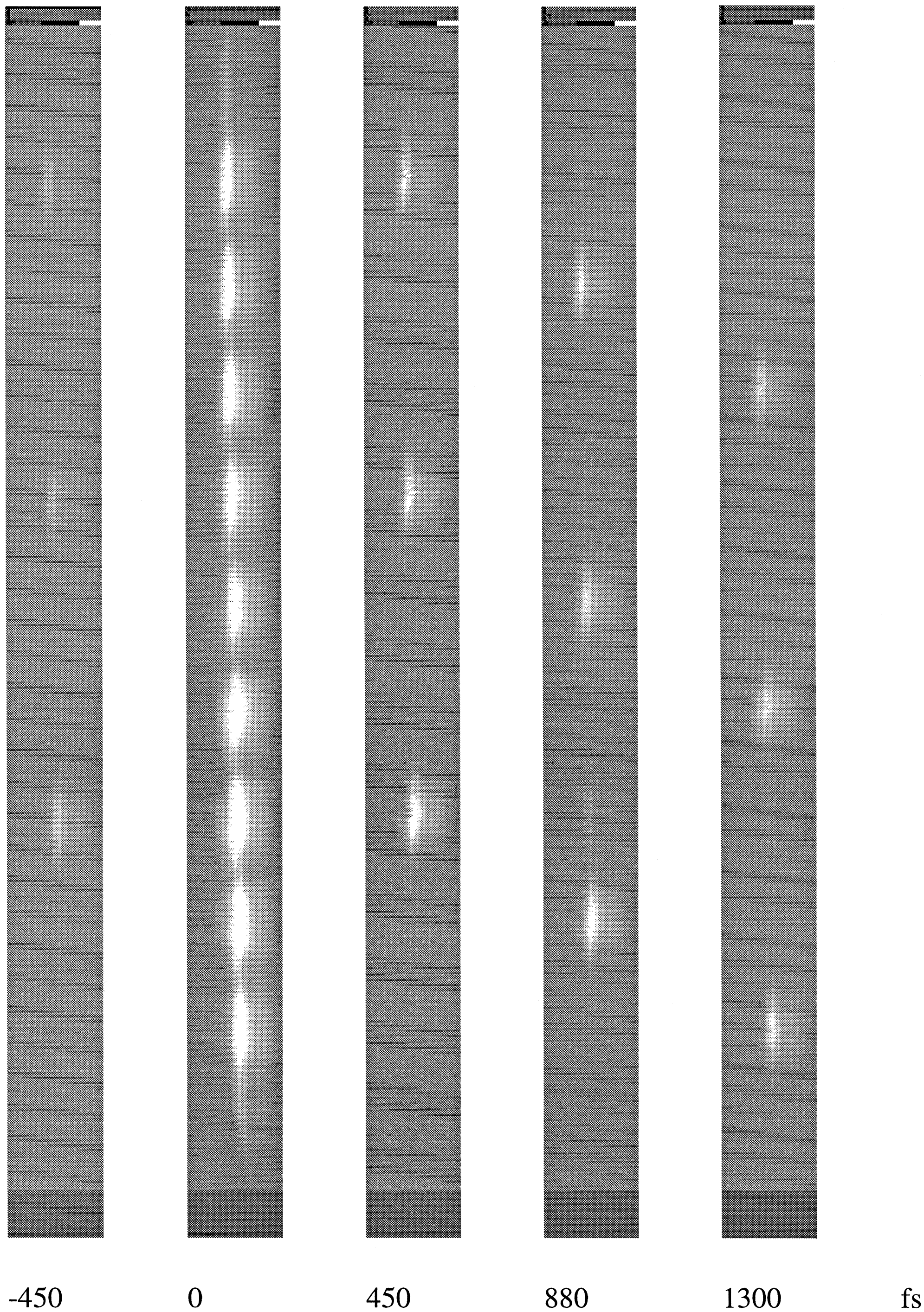

Fig. 3. CCD images of a multidimensional shaped waveform cross-correlated with an unshaped reference pulse at the delays shown. The zero time point corresponds to the zero-order temporal diffraction peak (second from left). Each spatial peak is ten mask pixels tall and is separated from adjacent peaks by ten fully darkened mask pixels (1 pixel ~ 24 μm).

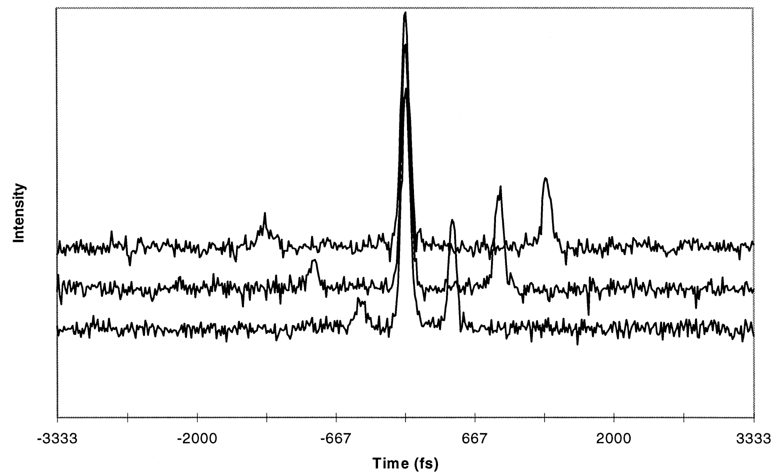

Fig. 4. Observed two-pulse sequences measured with the mask in one-dimensional mode (temporal shaping only). See Fig. 2 for theoretical values.

varying in only the horizontal dimension rather than in two dimensions. The spherical lens focuses each frequency component to a small spot, with the different frequency components separated horizontally and selectively filtered by the elements of the horizontal mask pattern to produce a single, temporally shaped output. In the present case the 2-D mask can be thought of as a series of horizontal patterns, one above the other, each of which is used to specify the temporal profile of the horizontal region of light incident upon it. Note that this picture is incomplete in that the output is spatially as well as temporally coherent, as discussed above.

Temporal-only pulse shaping was conducted first with permanent phase and amplitude mask patterns etched onto glass substrates. Automation was achieved by replacing the permanent masks with multielement liquid crystal spatial light modulators (SLMs) consisting of a horizontal row of separate pixels, each controlled independently to provide a specified amplitude modulation or phase retardation [2–4,7,8,11].

The 2-D mask used earlier consisted of permanent patterns etched onto a glass substrate [1]. As in temporal-only shaping, such a mask can be replaced by a multielement liquid crystal spatial light modulator (SLM) to provide automated waveform generation. The programmable mask used here is a Kopin Corp. (Taunton, MA) active matrix Super VGA liquid crystal display with 640×480 pixel resolution and individual pixels about 24 μm in size. A personal computer with a 24-bit SVGA display card and Microsoft Visual Basic drives the mask electronics. The 24-bit video adapter renders up to 256 grayscale intensity levels, and the mask electronics are analog. The incident pulse bandwidth is dispersed sufficiently to span all 640 horizontal pixels, but the spectrum does not appear to be severely truncated by the edges of the mask or its holder. The incident beam diameter determines how many pixels are spanned vertically; up to 190 pixels were used in these experiments.

The Kopin mask's twisted nematic design imposes some limitations in the types of waveforms it can generate because twisted nematic liquid crystals induce a polarization rotation, variable with the voltage applied across a pixel, that couples the amplitude and phase of the mask transfer function $m(x)$ [14]. In addition, the mask cannot generate a full 2π phase retardation (necessary for arbitrary waveform generation) but only $\sqrt{3}\,\pi/2$. Furthermore, the 'dead' spaces between adjacent pixels are rather large, yielding a 'fill factor' of only about 60%. Finally, only one mask was used although two are needed for independent phase and amplitude control. All these limitations notwithstanding, the high number of pixels on the present mask nevertheless allows sufficient freedom for generation of many practically useful waveforms. Once the above-mentioned difficulties are resolved, it will be possible to combine two masks (in a manner analogous to the development of high-resolution temporal pulse shapers [8,11]) to generate complicated, arbitrary waveforms that are spatially as well as temporally coherent. Moreover, unlike nematic single-dimensional spatial light modulators, this spatial light modulator and similar models are designed for commercial volume production.

When horizontally polarized light falls on the mask and a polarizer after the mask selects horizontally polarized light, the transmitted amplitude is [14]:

$$\frac{\sin\left[(\pi/2)\sqrt{1+3u^2}\right]}{\sqrt{1+3u^2}}, \tag{1}$$

with corresponding phase:

$$\exp\left(-iu\frac{\pi\sqrt{3}}{2}\right). \tag{2}$$

In this Letter, u is a dimensionless parameter varying between 0 and 1 that describes the orientation of the twisted nematic liquid crystal. With these u values, simulated annealing calculations can be used to find a mask pattern that generates a temporal pulse sequence with the desired intensities.

Our simulated annealing calculations use the Metropolis algorithm [15] to determine a mask pattern in the frequency domain which minimizes a heuristic potential energy function for the intensity in the time domain. A consequence of the coupled amplitude and phase of this mask's transfer function is that it is easy to form a second pulse on one side of the temporal zero order diffraction peak if the waveform on the other side of the zero order diffraction is allowed to vary freely. In Fig. 2, we show the results of calculations made under these restrictions.

These temporal pulse sequences may then be arranged to form a multidimensional waveform shaped in both space and time. Fig. 3 shows CCD images of SHG cross-correlation measurements of a multidimensional waveform based on the three temporal pulse sequences shown in Fig. 2. Each of the three temporal pulse sequences has been repeated in three independent strips, using ten rows of pixels per strip, at different vertical positions on the mask. Between pulse sequences, ten rows of pixels have been darkened by setting $u = 1$. The spatial and temporal evolution of the pulse sequence is best visualized with a motion picture. An MPEG movie of this pulse sequence, with one frame every 13.3 fs, has been produced and will be available over the Internet.

The temporal evolution of each vertically separated pulse sequence can best be measured by displaying the same mask pattern over all the rows of the mask so that it only shaped the temporal dimension. Observing the resulting SHG signal with a photodiode and lock-in detection yields experimental SHG intensity profiles of the two-pulse sequences (Fig. 4). Although theoretically the zero-order temporal diffraction peak and the delayed pulse are expected to have the same intensity (Fig. 2), that result is not observed, presumably due to calibration errors and variations across the mask.

In conclusion, we have demonstrated automated spatial (or wavevector) and temporal shaping of amplified ultrafast pulses using a commercially available spatial light modulator. Our results should encourage development of SLMs with higher fill factors, which would decrease the amount of light diffracted and reflected by the mask, and with nematic liquid crystals and sufficient phase retardation for greatly improved versatility in waveform specification.

Acknowledgements

This research was supported in part by NSF Grants No. CHE-9404548 and CHE-9713388.

References

[1] M.M. Wefers, K.A. Nelson, A.M. Weiner, Optics Lett. 21 (1996) 746.
[2] M.C. Nuss, R.L. Morrison, Optics Lett. 20 (1995) 740.
[3] J.P. Heritage, A.M. Weiner, R.N. Thurston, Optics Lett. 10 (1985) 609.
[4] A.M. Weiner, J.P. Heritage, E.M. Kirschner, J. Opt. Soc. Am. B 5 (1988) 1563.
[5] V. Binjrajka, C.-C. Chang, A.W.R. Emanuel, D.E. Leaird, A.M. Weiner, Optics Lett. 21 (1996) 1756.
[6] M. Haner, W.S. Warren, Appl. Phys. Lett. 52 (1988) 1458.
[7] A.M. Weiner, D.E. Leaird, J.S. Patel, J.R. Wullert, IEEE J. Quantum Electron. 28 (1992) 908.
[8] M.M. Wefers, K.A. Nelson, Optics Lett. 18 (1993) 2032.
[9] C.W. Hillegas, J.X. Tull, D. Goswami, D. Strickland, W.S. Warren, Optics Lett. 19 (1994) 737.
[10] A. Efimov, C. Shaffer, D.H. Reitze, J. Opt. Soc. Am. B 12 (1995) 1968.
[11] M.M. Wefers, K.A. Nelson, Optics Lett. 20 (1995) 1047.
[12] Y. Ding, R.M. Brubaker, D.D. Nolte, M.R. Melloch, A.M. Weiner, Optics Lett. 22 (1997) 718.
[13] L. Dhar, B. Burfeindt, K.A. Nelson, C.M. Foster, Ferroelectrics 164 (1996) 1.
[14] C.H. Gooch, H.A. Tarry, J. Phys. D 8 (1975) 1575.
[15] W.H. Press, S.A. Teukolsky, W.T. Vetterling, B.P. Flannery, Numerical Recipes in C, 2nd edn., Cambridge Univ. Press, New York, NY, 1992.